Reconstruction of Surfaces from Mixed Hydrocarbon and PEG Components in Water: Responsive Surfaces Aid Fouling Release

ARTICLE *in* BIOMACROMOLECULES · APRIL 2012

Impact Factor: 5.75 · DOI: 10.1021/bm300363g · Source: PubMed

8 AUTHORS, INCLUDING:

Youngjin Cho
Korea Institute of Science and Technology
23 PUBLICATIONS **224** CITATIONS
SEE PROFILE

Harihara Subramanian Sundaram
University of Washington Seattle
20 PUBLICATIONS **458** CITATIONS
SEE PROFILE

Michael Dimitriou
University of California, Santa Barbara
25 PUBLICATIONS **567** CITATIONS
SEE PROFILE

Christopher K Ober
Cornell University
587 PUBLICATIONS **15,905** CITATIONS
SEE PROFILE

Article

pubs.acs.org/Biomac

Reconstruction of Surfaces from Mixed Hydrocarbon and PEG Components in Water: Responsive Surfaces Aid Fouling Release

Youngjin Cho,[†] Harihara S. Sundaram,[†] John A. Finlay,[‡] Michael D. Dimitriou,[§] Maureen E. Callow,[‡] James A. Callow,[‡] Edward J. Kramer,[§,∥] and Christopher K. Ober*[,†]

[†]Department of Materials Science and Engineering, Cornell University, Ithaca, New York 14853, United States

[‡]School of Biosciences, The University of Birmingham, Birmingham B15 2TT, United Kingdom

[§]Department of Materials, University of California, Santa Barbara, California 93106, United States

[∥]Department of Chemical Engineering, University of California, Santa Barbara, California 93106, United States

Supporting Information

ABSTRACT: Coatings derived from surface active block copolymers (SABCs) having a combination of hydrophobic aliphatic (linear hydrocarbon or propylene oxide-derived groups) and hydrophilic poly(ethlyene glycol) (PEG) side chains have been developed. The coatings demonstrate superior performance against protein adsorption as well as resistance to biofouling, providing an alternative to coatings containing fluorinated side chains as the hydrophobe, thus reducing the potential environmental impact. The surfaces were examined using dynamic water contact angle, captive air-bubble contact angle, atomic force microscopy, X-ray photoelectron spectroscopy, and near-edge X-ray absorption fine structure analysis. The PS_{8K}-*b*-$P(E/B)_{25K}$-*b*-PI_{10K} triblock copolymer precursor (K3) initially dominated the dry surface. In contrast to previous studies with mixed fluorinated/PEG surfaces, these new materials displayed significant surface changes after exposure to water that allowed fouling resistant behavior. PEG groups buried several nanometers below the surface in the dry state were able to occupy the coating surface after placement in water. The resulting surface exhibits a very low contact angle and good antifouling properties that are very different from those of K3. The surfaces are strongly resistant to protein adsorption using bovine serum albumin as a standard protein challenge. Biofouling assays with sporelings of the green alga *Ulva* and cells of the diatom *Navicula* showed the level of adhesion was significantly reduced relative to that of a PDMS standard and that of the triblock copolymer precursor of the SABCs.

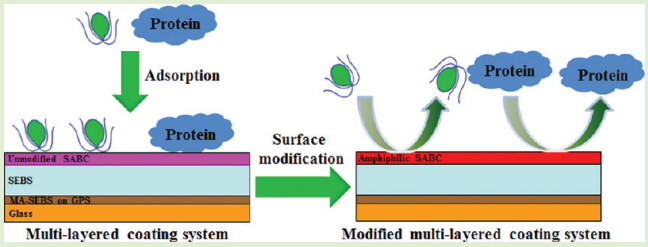

INTRODUCTION

Biofouling, which consists of the accumulation and adhesion of various microorganisms, proteins, plants, and animals on a submerged surface, is a principal problem in many areas of the marine and aquatic industries, as well as on medical implants, and biodevices that contact living systems. In particular, the effects of biofouling in the marine industry, such as accumulation on the hulls of ships, lead to increased consumption of fuel, lower obtainable speeds, and higher maintenance costs.[1,2] Although antifouling paints containing tributyltin, copper, and organic cobiocides have been used to mitigate fouling, some active ingredients are now banned or likely to be more severely regulated in the future, driven by environmental concerns.[3,4] Therefore, current research in antifouling coatings is focused on developing alternative environmentally benign materials.[5−8] New strategic materials against biofouling must possess antifouling properties that inhibit the settling stages of fouling organisms and/or possess fouling-release properties, i.e., low adhesion strength of the organisms that have colonized the surface.

The main strategic approaches of recent research in antifouling and fouling-release applications involve the use of homogeneous surfaces such as hydrophilic, hydrophobic, or amphiphilic surfaces, heterogeneous surfaces such as mixed or patterned surfaces, and three-dimensional surfaces such as topographically patterned surfaces.[9−11] Hydrophilic surfaces for biofouling prevention have generally focused on the use of poly(ethylene glycol) (PEG), known for its exceptional resistance to protein adsorption and cell adhesion.[12−14] Hydrophobic surfaces such as those formed from poly(dimethyl siloxane) (PDMS)[15−17] or block copolymers containing fluorinated side chains[18,19] have demonstrated excellent fouling-release properties as a result of their low surface energy in conjunction with their low elastic modulus.[20,21] However, as demonstrated in prior work, hydrophobic or hydrophilic surfaces alone are limited in biofouling control because they are each effective against only a limited number of species.[19] As an alternative, amphiphilic materials containing both hydrophilic and hydrophobic groups have been shown to inhibit settlement and improve fouling

Received: March 6, 2012
Revised: April 21, 2012
Published: April 24, 2012

release (i.e., reduce adhesion strength) of a range of biofoulers.[22] Amphiphilic hyperbranched polymers containing both fluorinated and PEGylated groups were shown to have superior performance in both protein adsorption and fouling release of algae at the optimal composition of hydrophobic and hydrophilic segments.[23] Several surface active block copolymers derived from perfluorinated and PEGylated amphiphilic side chains were capable of resisting and releasing both the green alga *Ulva* and the diatom *Navicula* as well as deterring barnacle settlement.[24,25] Martinelli et al. reported the fouling-release performance of *Ulva* using similar fluorinated surface active block copolymers.[26] Recently, Park et al. demonstrated superior antifouling and fouling-release properties on heterogeneous surfaces of surface active block copolymers with grafted mixed fluorinated and PEG side chains.[27] Martinelli et al. also reported the excellent fouling-release performance of an amphiphilic diblock copolymer containing a polysiloxane and PEGylated fluoroalkyl groups.[28] These results strongly demonstrate the potential of amphiphilic surfaces to combat marine biofouling, irrespective of whether they have single moieties that contain both polar and nonpolar groups or whether these polar and nonpolar groups are separately incorporated along the outermost polymer block backbone. In such amphiphilic materials, the presence of fluorinated groups allows the colocation of PEG groups in the near surface region during the coating process.

To date, almost all antifouling surface systems have relied on fluorinated segments as the hydrophobic moiety in an amphiphilic system. However, fluorinated compounds with more than four consecutive CF_2 units have been shown to potentially bioaccumulate in mammalian blood and are thus recognized as environmentally hazardous materials.[29−31] Therefore, fluorine-free materials with comparable properties are being evaluated for antifouling and fouling-release applications. We have developed fluorine-free surface active block copolymers derived from amphiphilic side chains with PEG and alkyl segments.[32] These fluorine-free surface active block copolymers (SABCs) containing alkyl hydrophobic segments as a replacement for fluorinated chains demonstrated excellent performance against both *Ulva* and the diatom *Navicula*.

Following this success, we have now systematically expanded our study of heterogeneous surfaces to different fluorine-free hydrophobic groups in combination with hydrophilic PEG. We report here the synthesis, characterization, and biofouling performance of fluorine-free, amphiphilic SABCs derived from the mixture of alkyl or polypropylene glycol (PPG) hydrophobic segments and PEG hydrophilic side chains to a polystyrene-*block*-poly(ethylene-*ran*-butylene)-*block*-poly(isoprene) [PS-*b*-P(E/B)-*b*-PI] triblock copolymer precursor. We also report the "reconstruction" of these mixed amphiphilic surfaces in water. Surfaces of the fluorine-free, mixed amphiphilic SABCs were characterized using dynamic water contact angle, captive air-bubble contact angle, atomic force microscopy (AFM), X-ray photoelectron spectroscopy (XPS), and near-edge X-ray absorption fine structure (NEXAFS) analysis. The surfaces of the polymer films were hydrophilic in aqueous media because of surface reconstruction bringing PEG groups to the surface that are buried several nanometers in the dry state, despite the absence of fluorinated groups that we have used previously to draw PEG to the surface region.[22] The adhesion strength of both sporelings (young plants) of the green alga *Ulva* and cells of the diatom *Navicula* and the resistance to protein adsorption were evaluated on the amphiphilic SABCs modified with mixed hydrophobic and hydrophilic side chains.

EXPERIMENTAL SECTION

Materials. The polystyrene$_{8K}$-*block*-poly(ethylene-*ran*-butylene)$_{25K}$-*block*-polyisoprene$_{10K}$ [PS_{8K}-*b*-P(E/B)$_{25K}$-*b*-PI_{10K}] triblock copolymer precursor was produced using anionic polymerization and subsequent catalytic hydrogenation by Kraton Polymers to facilitate preparation of SABCs. Polystyrene-*block*-poly(ethylene-*ran*-butylene)-*block*-polystyrene (SEBS) triblock thermoplastic elastomers (Kraton product no. MD6945) and SEBS grafted with maleic anhydride (MA-SEBS, Kraton product no. FG1901X) were kindly provided by Kraton Polymers. 3-Chloroperoxybenzoic acid [*m*-CPBA, ClC_6H_4COOOH, formula weight (FW) of 172.57, 77%], boron trifluoride diethyl etherate [$BF_3{\cdot}Et_2O$, $BF_3{\cdot}O(CH_2CH_3)_2$, FW of 141.93, 99.9%], 1-octadecanol, 1-hexanol, polyethylene glycol methyl ether ($M_n \sim 350$), polyethylene glycol methyl ether ($M_n \sim 550$), polyethylene glycol methyl ether [$CH_3(OCH_2CH_2)_nOH$, $n \sim 16$, $M_n \sim 750$], polyethylene glycol methyl ether ($M_n \sim 1000$), polypropylene glycol butyl ether $CH_3CH_2CH_2CH_2[OCH_2CH(CH_3)]_nOH$, $n \sim 16$, $M_n \sim 1000$}, and anhydrous chloroform ($CHCl_3$) were purchased from Sigma Aldrich and used as received without further purification. Cyclohexane, dichloromethane (CH_2Cl_2), methanol (CH_3OH), toluene, 6.25 N sodium hydroxide (NaOH), 96% sulfuric acid (H_2SO_4), 30 wt % hydrogen peroxide (H_2O_2) in water, 95% ethanol (CH_3CH_2OH), and all other reagents were used as received. 3-(Glycidoxypropyl)-trimethoxysilane (GPS, 99%) was purchased from Gelest and used as received. The polystyrene standards (molecular mass of 1000−1000000 Da) were purchased from Polymer Standards Service, Inc.

Synthesis of the Amphiphilic SABCs with Mixed Hydrophobic and Hydrophilic Side Chains. The detailed synthesis and characterization of epoxidized PS_{8K}-*b*-P(E/B)$_{25K}$-*b*-PI_{10K} has been described previously.[32] The amphiphilic SABCs with grafted mixed hydrophobic and hydrophilic side chains were produced through a boron-catalyzed ring opening reaction with various mixtures of hydrophobic 1-hexanol, 1-octadecanol, or PPG alcohols and hydrophilic PEG alcohols in a fashion similar to that previously reported.[27] The resultant SABCs were precipitated into methanol. The SABCs were collected by filtration and subsequently reprecipitated three times into methanol from chloroform to remove additional residual surface active side chain alcohol precursors. Finally, the compounds were dried under reduced pressure at room temperature for 48 h to fully remove residual solvent.

Epoxidized PS_{8K}-*b*-P(E/B)$_{25K}$-*b*-PI_{10K}: ^{1}H NMR (300 MHz, $CDCl_3$) δ 6.58, 7.10, (5H, styrene), 2.68 [br s, 1H, epoxidized isoprene, -$CH_2HCOC(CH_3)CH_2$-], 0.80, 1.08, 1.26, 1.47, 1.57 (backbone); IR (dry film) υ_{max} 2925, 2850 (C−H stretching), 1600, 1470 (C═C, aromatic), 1070 (C−O stretching), 880 (C−O−C stretching), 700 cm^{-1} (C−H bending, aromatic).

PS_{8K}-*b*-P(E/B)$_{25K}$-*b*-PI_{10K} functionalized with PEG550 side chains: ^{1}H NMR (300 MHz, $CDCl_3$) δ 6.56, 7.08 (5H, styrene), 3.63 [br s, -(OCH_2CH_2)-], 3.38 (s, -OCH_3), 2.24 (s, -OH), 0.83, 1.06, 1.24, 1.80 (br, polymer backbone); IR (dry film) υ_{max} 3350 (O−H stretching), 2935, 2865 (C−H stretching), 1600, 1455 (C═C, aromatic), 1375 (C−H bending), 1120 (C−O stretching), 765, 700 cm^{-1} (C−H bending, aromatic). Elemental analysis: C (76.80%), H (12.44%), O (10.76%).

PS_{8K}-*b*-P(E/B)$_{25K}$-*b*-PI_{10K} functionalized with 1-octadecanol side chains: ^{1}H NMR (300 MHz, $CDCl_3$) δ 6.58, 7.10 (5H, styrene), 3.64 [br s, -$OCH_2(CH_2)$-], 0.82, 1.05, 1.24, 1.81 [br, $CH_3(CH_2)_{16}CH_2$- of 1-octadecanol side chain and polymer backbone]; IR (dry film) υ_{max} 3480 (O−H stretching), 2930, 2855 (C−H stretching), 1600, 1460 (C═C, aromatic), 1380 (C−H bending), 1115 (C−O stretching), 765, 700 cm^{-1} (C−H bending, aromatic). Elemental analysis: C (79.92%), H (13.08%), O (7.00%).

PS_{8K}-*b*-P(E/B)$_{25K}$-*b*-PI_{10K} functionalized with both PEG550 (75% by mole feed ratio) and 1-octadecanol (25% by mole feed ratio) side chains: ^{1}H NMR (300 MHz, $CDCl_3$) δ 6.59, 7.09 (5H, styrene), 3.66 [br s, -(OCH_2CH_2)- and -$OCH_2(CH_2)$-], 3.43 (s, -OCH_3), 0.82, 1.06,

1.25, 1.82 [br, $CH_3(CH_2)_{16}CH_2$- of 1-octadecanol side chain and polymer backbone]. Elemental analysis: C (76.42%), H (11.44%), O (12.14%).

PS_{8K}-*b*-$P(E/B)_{25K}$-*b*-PI_{10K} functionalized with both PEG550 (50% by mole feed ratio) and 1-octadecanol (50% by mole feed ratio) side chains: ^{1}H NMR (300 MHz, $CDCl_3$) δ 6.60, 7.09 (5H, styrene), 3.62 [br s, -(OCH_2CH_2)- and -$OCH_2(CH_2)$-], 3.42 (s, -OCH_3), 0.82, 1.06, 1.23, 1.84 [br, $CH_3(CH_2)_{16}CH_2$- of 1-octadecanol side chain and polymer backbone]; IR (dry film) υ_{max} 3485 (O−H stretching), 2935, 2865 (C−H stretching), 1605, 1465 (C═C, aromatic), 1380 (C−H bending), 1125 (C−O stretching), 760, 705 cm^{-1} (C−H bending, aromatic). Elemental analysis: C (77.09%), H (12.38%), O (10.53%).

PS_{8K}-*b*-$P(E/B)_{25K}$-*b*-PI_{10K} functionalized with both PEG550 (25% by mole feed ratio) and 1-octadecanol (75% by mole feed ratio) side chains: ^{1}H NMR (300 MHz, $CDCl_3$) δ 6.57, 7.09 (5H, styrene), 3.64 [br s, -(OCH_2CH_2)- and -$OCH_2(CH_2)$-], 3.39 (s, -OCH_3), 0.80, 1.06, 1.25, 1.81 [br, $CH_3(CH_2)_{16}CH_2$- of 1-octadecanol side chain and polymer backbone]. Elemental analysis: C (78.23%), H (12.35%), O (9.42%).

PS_{8K}-*b*-$P(E/B)_{25K}$-*b*-PI_{10K} functionalized with both 1-hexanol (50% by mole feed ratio) and PEG350 (50% by mole feed ratio) side chains: ^{1}H NMR (300 MHz, $CDCl_3$) δ 6.61, 7.09 (5H, styrene), 3.65 [br s, -(OCH_2CH_2)- and -$OCH_2(CH_2)$-], 3.38 (s, -OCH_3), 0.81, 1.05, 1.25, 1.82 [br, $CH_3(CH_2)_{16}CH_2$- of 1-hexanol side chain and polymer backbone]; IR (dry film) υ_{max} 3465 (O−H stretching), 2925, 2860 (C−H stretching), 1615, 1465 (C═C, aromatic), 1395 (C−H bending), 1125 (C−O stretching), 760, 705 cm^{-1} (C−H bending, aromatic). Elemental analysis: C (78.37%), H (13.01%), O (8.62%).

PS_{8K}-*b*-$P(E/B)_{25K}$-*b*-PI_{10K} functionalized with both 1-hexanol (50% by mole feed ratio) and PEG550 (50% by mole feed ratio) side chains: ^{1}H NMR (300 MHz, $CDCl_3$) δ 6.59, 7.09 (5H, styrene), 3.64 [br s, -(OCH_2CH_2)- and -$OCH_2(CH_2)$-], 3.39 (s, -OCH_3), 0.80, 1.07, 1.25, 1.85 [br, $CH_3(CH_2)_{16}CH_2$- of 1-hexanol side chain and polymer backbone]. Elemental analysis: C (79.02%), H (12.48%), O (8.50%).

PS_{8K}-*b*-$P(E/B)_{25K}$-*b*-PI_{10K} functionalized with both 1-hexanol (50% by mole feed ratio) and PEG750 (50% by mole feed ratio) side chains: ^{1}H NMR (300 MHz, $CDCl_3$) δ 6.59, 7.09 (5H, styrene), 3.64 [br s, -(OCH_2CH_2)- and -$OCH_2(CH_2)$-], 3.39 (s, -OCH_3), 0.82, 1.05, 1.25, 1.89 [br, $CH_3(CH_2)_{16}CH_2$- of 1-hexanol side chain and polymer backbone]. Elemental analysis: C (80.98%), H (13.26%), O (5.76%).

PS_{8K}-*b*-$P(E/B)_{25K}$-*b*-PI_{10K} functionalized with both 1-hexanol (50% by mole feed ratio) and PEG1000 (50% by mole feed ratio) side chains: ^{1}H NMR (300 MHz, $CDCl_3$) δ 6.59, 7.09 (5H, styrene), 3.64 [br s, -(OCH_2CH_2)- and -$OCH_2(CH_2)$-], 3.39 (s, -OCH_3), 0.82, 1.05, 1.25, 1.85 [br, $CH_3(CH_2)_{16}CH_2$- of 1-hexanol side chain and polymer backbone]. Elemental analysis: C (79.98%), H (12.13%), O (7.89%).

PS_{8K}-*b*-$P(E/B)_{25K}$-*b*-PI_{10K} functionalized with both 1-octadecanol (50% by mole feed ratio) and PEG350 (50% by mole feed ratio) side chains: ^{1}H NMR (300 MHz, $CDCl_3$) δ 6.58, 7.09 (5H, styrene), 3.64 [br s, -(OCH_2CH_2)- and -$OCH_2(CH_2)$-], 3.38 (s, -OCH_3), 0.81, 1.05, 1.25, 1.84 [br, $CH_3(CH_2)_{16}CH_2$- of 1-octadecanol side chain and polymer backbone]; IR (dry film) υ_{max} 3465 (O−H stretching), 2945, 2835 (C−H stretching), 1610, 1466 (C═C, aromatic), 1380 (C−H bending), 1125 (C−O stretching), 765, 705 cm^{-1} (C−H bending, aromatic). Elemental analysis: C (78.82%), H (12.63%), O (8.55%).

PS_{8K}-*b*-$P(E/B)_{25K}$-*b*-PI_{10K} functionalized with both 1-octadecanol (50% by mole feed ratio) and PEG550 (50% by mole feed ratio) side chains: ^{1}H NMR (300 MHz, $CDCl_3$) δ 6.59, 7.09 (5H, styrene), 3.64 [br s, -(OCH_2CH_2)- and -$OCH_2(CH_2)$-], 3.39 (s, -OCH_3), 0.82, 1.07, 1.25, 1.82 [br, $CH_3(CH_2)_{16}CH_2$- of 1-octadecanol side chain and polymer backbone]. Elemental analysis: C (76.08%), H (12.21%), O (11.71%).

PS_{8K}-*b*-$P(E/B)_{25K}$-*b*-PI_{10K} functionalized with both 1-octadecanol (50% by mole feed ratio) and PEG750 (50% by mole feed ratio) side chains: ^{1}H NMR (300 MHz, $CDCl_3$) δ 6.59, 7.09 (5H, styrene), 3.64 [br s, -(OCH_2CH_2)- and -$OCH_2(CH_2)$-], 3.39 (s, -OCH_3), 0.82, 1.07, 1.24, 1.84 [br, $CH_3(CH_2)_{16}CH_2$- of 1-octadecanol side chain and polymer backbone]. Elemental analysis: C (75.86%), H (11.53%), O (12.61%).

PS_{8K}-*b*-$P(E/B)_{25K}$-*b*-PI_{10K} functionalized with both 1-octadecanol (50% by mole feed ratio) and PEG1000 (50% by mole feed ratio) side chains: ^{1}H NMR (300 MHz, $CDCl_3$) δ 6.59, 7.10 (5H, styrene), 3.64 [br s, -(OCH_2CH_2)-], 3.38 (s, -OCH_3), 0.82, 1.07, 1.25, 1.88 [br, $CH_3(CH_2)_{16}CH_2$- of 1-octadecanol side chain and polymer backbone]. Elemental analysis: C (77.74%), H (12.19%), O (10.07%).

PS_{8K}-*b*-$P(E/B)_{25K}$-*b*-PI_{10K} functionalized with PPG1000 side chains: ^{1}H NMR (300 MHz, $CDCl_3$) δ 6.6, 7.1 (5H, styrene), 3.55 [br, m, -$O(CH_3)$CH-C***H***$_2$O-], 3.40 [br, -O-(CH_3)C***H***-CH_2O-], 0.8, 1.14, 1.24, 1.8 [br, -O-(C***H***$_3$)$CHCH_2$O- and polymer backbone].

PS_{8K}-*b*-$P(E/B)_{25K}$-*b*-PI_{10K} functionalized with PEG750 side chains: ^{1}H NMR (300 MHz, $CDCl_3$) δ 6.6, 7.1 (5H, styrene), 3.6 (br, s, -OC***H***$_2$C***H***$_2$-O-), 3.40 (s, -OC***H***$_3$), 0.8, 1.14, 1.24, 1.8 (br, polymer backbone).

PS_{8K}-*b*-$P(E/B)_{25K}$-*b*-PI_{10K} functionalized with both PPG1000 (50% by mole feed ratio) and PEG750 (50% by mole feed ratio) side chains: ^{1}H NMR (300 MHz, $CDCl_3$) δ 6.6, 7.1 (5H, styrene), 3.55 [br, m, -$O(CH_3)$CH-C***H***$_2$O- and -OC***H***$_2$C***H***$_2$-O], 3.40 [br, -O-(CH_3)C***H***-CH_2O-], 0.8, 1.14, 1.24, 1.8 [br, -O-(C***H***$_3$)$CHCH_2$O- and polymer backbone].

Characterization. ^{1}H NMR spectra were recorded using a Varian Gemini spectrometer with deuterated chloroform as the solvent. The FTIR spectra of the polymers cast as films from a tetrahydrofuran (THF) solution on sodium chloride plates were recorded using a Mattson 2020 Galaxy Series FTIR spectrometer. Elemental analysis for C, H, and O weight fractions of the surface active block copolymers was performed by Quantitative Technologies, Inc. (QTI). Gel permeation chromatography (GPC) of a THF solution of polymers (1 mg/mL) was conducted using four Waters Styragel HT columns operating at 40 °C in conjunction with Waters 490 ultraviolet (λ = 254 nm) and Waters 410 refractive index detectors. The molecular mass range of the columns was from 500 to 10^7 Da. THF was used as the eluent at a flow rate of 1 mL/min, and toluene was used as a marker for flow calibration. The gel permeation chromatograph was calibrated using a series of low-polydispersity polystyrene standards.

Water contact angles were measured using a contact angle goniometer (AST Products, Inc., model VCA Optima XE) at room temperature. Dynamic water contact angle measurements were performed via the addition and retraction of a small drop of water (2 μL) on the surface. The advancing and receding contact angles were digitally recorded, and image analysis software was used to measure the angles. Three measurements each for two different areas on the surface were taken.

The contact angle of an air bubble on the surface immersed in MilliQ water was measured using the captive bubble method. An air bubble, on the snapped-off tip of a 22 gauge stainless steel syringe needle (0.7 mm outside diameter and 0.4 mm inside diameter), was contacted by the surface immersed in water, and the contact angle was measured. The angle between the surface and the air bubble on the water side was measured. Therefore, a low captive-bubble contact angle indicates a hydrophilic surface, while a higher angle indicates a more hydrophobic surface.

Tapping-mode AFM measurements were taken using a Digital Instruments Dimension 3000 atomic force microscope. Phase-contrast images were collected over 1 μm × 1 μm regions to reveal the surface morphology. Images were collected using Applied Nanostructures long cantilevers (ACL) at 1.5 Hz.

XPS measurements were performed using a Kratos Axis Ultra Spectrometer (Kratos Analytical, Manchester, U.K.) with a monochromatic Al Kα X-ray source (1486.6 eV) operating at 225 W under a vacuum of 1.0×10^{-8} Torr. Charge compensation was achieved via the injection of low-energy electrons into the magnetic lens of the electron spectrometer. The pass energy of the analyzer was set at 40 eV for high-resolution spectra and 80 eV for survey scans, with energy resolutions of 0.05 and 1 eV, respectively. The spectra were analyzed using Casa XPS version 2.3.12Dev4. The C−C peak at 285 eV was used as the reference for binding energy calibration.

Near-edge X-ray absorption fine structure (NEXAFS) measurements were taken at the U7A NIST/Dow materials characterization end-station at the National Synchrotron Light Source at Brookhaven

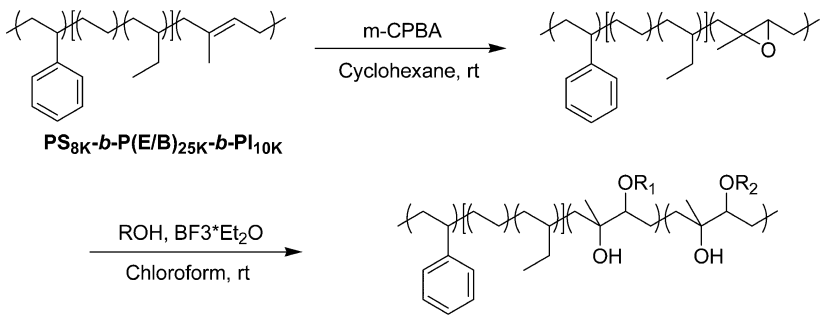

Figure 1. Synthetic scheme of fluorine-free, amphiphilic surface active block copolymers (SABCs) with mixed hydrophobic and hydrophilic side chains. R_1OH is 1-hexanol, 1-octadecanol, or PPG butyl ether ($M_n \sim 1000$); R_2OH is PEG methyl ether ($M_n \sim 350$, 550, 750, or 1000 g/mol).

National Laboratory (BNL). The general underlying principles of NEXAFS and a description of the beamline at BNL have been reported previously.[33,34] The X-ray beam was elliptically polarized (polarization factor of 0.85), with the electric field vector dominantly in the plane of the storage ring. The photon flux was approximately 1×10^{11} photons/s at a typical storage ring current of 750 mA. A spherical grating monochromator was used to obtain monochromatic soft X-rays with an energy resolution of 0.2 eV. The C 1s NEXAFS spectra were acquired for incident photon energy in the range of 270−320 eV. The angle of incidence of the X-ray beam, measured from the sample surface, was 50°. The partial-electron-yield (PEY) signal was collected using a channeltron electron multiplier with an adjustable entrance grid bias (EGB) of −150 V. The channeltron PEY detector was positioned at an angle of 35° above the equatorial plane of the sample chamber and at an angle of 36° in that plane relative to the incoming X-ray beam.[35] We normalized the PEY C 1s spectra by subtracting a linear pre-edge baseline and setting the edge jump to unity at 320 eV. The photon energy was calibrated by adjusting the peak position of the lowest π^* phenyl resonance from polystyrene to 285.5 eV.

Preparation of Surfaces for Characterization and Biofouling Assays. Surfaces for dynamic water contact angle, captive air-bubble contact angle, AFM, XPS, and NEXAFS analysis and biofouling assays were prepared on glass slides by spray-coating.[36] The glass slides were cleaned by immersion in a 7:3 (v/v) mixture of concentrated H_2SO_4 and a 30 wt % H_2O_2 solution and then rinsed with water, dried, and subsequently functionalized with a 4% (w/v) solution of 3-(glycidoxy)trimethoxysilane in ethanol. The silane was cured by heating the functionalized glass slides to 110 °C for 2 h followed by slow cooling to room temperature. This epoxy-containing silane served as an adhesion promoter for the initial SEBS layer spin coated from a 7% (w/v) SEBS solution in toluene (5% Kraton FG-1901X and 2% Kraton MD 6945). The thickness of the SEBS base layer was then built up through successive spin coating of a 12% (w/v) SEBS solution (Kraton MD 6945) in toluene three times. Finally, the layer of SABC was deposited on top of the SEBS base layer through spray coating from a 3% (w/v) solution in toluene. The coated glass slides were annealed at 60 °C for 24 h and 120 °C for 24 h. The SEBS base layer was ∼500 μm thick, and the SABC layer deposited via spray coating was ∼20 μm thick. Polymer surfaces are named according to the feed ratio of the side chain. O*x*P*y* represents the PS_{8K}-*b*-$P(E/B)_{25K}$-*b*-PI_{10K} with an *x* feed ratio of 1-octadecanol and a *y* feed ratio of PEG550. PG*x*EG*y* represents the PS_{8K}-*b*-$P(E/B)_{25K}$-*b*-PI_{10K} with an *x* feed ratio of PPG1000 and a *y* feed ratio of PEG750. The other polymer surfaces containing the different aliphatic and PEG alcohols in a 50:50 feed ratio are named according to the side chains. For example, HP350 represents the PS_{8K}-*b*-$P(E/B)_{25K}$-*b*-PI_{10K} with 1-hexanol and PEG350. OP1000 represents the PS_{8K}-*b*-$P(E/B)_{25K}$-*b*-PI_{10K} with 1-octadecanol and PEG1000.

A poly(dimethylsiloxane) elastomer (PDMSe) (Silastic T2, Dow Corning), known to possess good fouling-release properties for sporelings of *Ulva* and prepared as described by Schumacher et al.,[37] was included in the release assays as a standard. Kraton MD6945 was used as the thermoplastic elastomer base layer in the multilayer coating to produce an underlayer with a relatively low Young's modulus that has been shown to be important for the best fouling-release performance.[26] Films of the PS_{8K}-*b*-$P(E/B)_{25K}$-*b*-PI_{10K} triblock copolymer precursor were also included as controls for both biofouling and protein absorption tests. This film was denoted as K3.

Protein Adsorption Test. A 0.5 mg quantity of fluorescein isothiocyanate-labeled bovine serum albumin (BSA-FITC) was dissolved in 5 mL of a PBS buffer solution. The slides were incubated in the BSA-FITC solution in a dark room for 2 h, thoroughly rinsed with deionized water, and then dried with a flow of N_2 gas. To measure the fluorescence intensity, fluorescence microscopy (excitation wavelength of 450 nm and emission filter set to 550 nm) was performed using an Olympus BX51 upright microscope with a 40× UPlan Fluorite dry objective (N.A. 0.75). Images were acquired using a Roper Cool Snap HQ CCD camera and Image Pro image acquisition and processing software.

Strength of Attachment of Sporelings of *Ulva*. Nine replicate test samples were immersed in 5 L of circulating deionized water at ∼20 °C for 48 h. The slides were equilibrated in artificial seawater 1 h prior to the start of the experiments. Zoospores were released from fertile plants of *Ulva linza* and prepared for assay as described previously.[38] Ten milliliters of a zoospore suspension (1×10^6 spores/mL) was pipetted into nine individual compartments of Quadriperm polystyrene culture dishes (Greiner Bio-One), each containing a test slide. The test slides were incubated in the dark at ∼20 °C for 1 h and washed in seawater to remove zoospores that had not settled. Three slides were fixed using 2.5% glutaraldehyde in seawater, and these replicates were used to quantify the density of zoospores attached to the surfaces as previously reported.[39]

Sporelings of *Ulva* (young plants) were cultured on six replicates of each coating.[40] After being washed, the samples were transferred to dishes containing nutrient-enriched seawater for 7 days. Growth was estimated by direct measurement of fluorescence from chlorophyll contained within the chloroplasts of the sporelings using a Tecan plate reader (GENios Plus).[41] Fluorescence was recorded as relative fluorescence units (RFU) from direct readings. The slides (six replicates) were read from the top, 70 readings per slide, taken from the central area (5 cm^2). The strength of attachment of the sporelings was determined by jet washing using a water jet.[42] The range of impact pressures used was chosen to provide the maximal amount of information about the strength of attachment of the sporelings. After exposure to the water jet, RFU readings were again taken from the central part of the slide. The percentage removal was calculated from the mean RFU reading before and after exposure to the water jet. From curves of the percentage removal versus impact pressure, the critical water pressure (kilopascals) required to remove 50% of the sporelings was derived.

Attachment and Adhesion Strength of Cells of the Diatom *Navicula*. Cells of the diatom *Navicula* were cultured in F/2 medium contained in 250 mL conical flasks. A log-phase suspension of cells was diluted to give a suspension with a chlorophyll content of approximately 0.25 μg/mL. Ten milliliters of cell suspension was added to individual compartments of Quadriperm polystyrene culture dishes (Greiner Bio-One), each containing a test slide, prepared as

dx.doi.org/10.1021/bm300363g | *Biomacromolecules* 2012, 13, 1864−1874

Table 1. Percentage Attachment of Side Chains and Dynamic Water Contact Angles of the Amphiphilic Triblock Copolymer Surfaces with Grafted 1-Octadecanol and PEG550 Side Chains

block copolymer	surface nomenclature[a]	% attachment of $C_{18}OH$	% attachment of PEG550	overall % attachment	$\theta_{w,ad}$	$\theta_{w,re}$	hysteresis
SEBS	SEBS	–	–	–	129.7 ± 1.2	56.5 ± 4.2	73.2
PS_{8K}-*b*-$P(E/B)_{25K}$-*b*-PI_{10K}	K3	–	–	–	116.3 ± 0.8	59.4 ± 2.4	56.9
PS_{8K}-*b*-$P(E/B)_{25K}$-*b*-PI_{10K}-octadecanol100-PEG0	O100P0	38.3		38.3	119.9 ± 1.7	42.7 ± 3.3	77.2
PS_{8K}-*b*-$P(E/B)_{25K}$-*b*-PI_{10K}-octadecanol75-PEG25	O75P25	15.2	6.1	21.3	119.4 ± 0.9	34.9 ± 1.1	84.5
PS_{8K}-*b*-$P(E/B)_{25K}$-*b*-PI_{10K}-octadecanol50-PEG50	O50P50	13.4	11.7	25.1	118.9 ± 1.4	34.6 ± 3.1	84.3
PS_{8K}-*b*-$P(E/B)_{25K}$-*b*-PI_{10K}-octadecanol25-PEG75	O25P75	7.4	21.5	28.9	118.0 ± 1.2	32.7 ± 2.0	85.3
PS_{8K}-*b*-$P(E/B)_{25K}$-*b*-PI_{10K}-octadecanol0-PEG100	O0P100		34.2	34.2	115.4 ± 1.4	32.3 ± 0.9	83.1

[a]Polymer surfaces are named according to the feed ratio of the side chain. O*x*P*y* represents the PS_{8K}-*b*-$P(E/B)_{25K}$-*b*-PI_{10K} with an *x* feed ratio of 1-octadecanol and a *y* feed ratio of PEG550.

Table 2. Percentage Attachment of Side Chains and Dynamic Water Contact Angles of the Amphiphilic Triblock Copolymer Surfaces with Grafted 1-Hexanol/1-Octadecanol and PEG Side Chains of Different Lengths

block copolymer	surface nomenclature[a]	% attachment of C_6/$C_{18}OH$	% attachment of PEGs	overall % attachment	$\theta_{w,ad}$	$\theta_{w,re}$	hysteresis
PS_{8K}-*b*-$P(E/B)_{25K}$-*b*-PI_{10K}-hexanol-PEG350	HP350	10.5	12.9	23.4	117.8 ± 0.9	36.0 ± 1.2	81.8
PS_{8K}-*b*-$P(E/B)_{25K}$-*b*-PI_{10K}- hexanol-PEG550	HP550	9.7	10.1	19.8	115.3 ± 1.5	32.6 ± 2.9	82.7
PS_{8K}-*b*-$P(E/B)_{25K}$-*b*-PI_{10K}- hexanol-PEG750	HP750	10.4	12.4	22.8	113.8 ± 1.1	29.5 ± 0.9	84.3
PS_{8K}-*b*-$P(E/B)_{25K}$-*b*-PI_{10K}- hexanol-PEG1000	HP1000	15.9	13.0	28.9	113.0 ± 0.2	23.7 ± 1.5	89.3
PS_{8K}-*b*-$P(E/B)_{25K}$-*b*-PI_{10K}-octadecanol-PEG350	OP350	11.2	10.7	21.9	117.2 ± 1.1	42.3 ± 2.2	74.9
PS_{8K}-*b*-$P(E/B)_{25K}$-*b*-PI_{10K}-octadecanol-PEG550	OP550	13.1	11.8	24.9	115.6 ± 1.4	39.9 ± 2.4	75.7
PS_{8K}-*b*-$P(E/B)_{25K}$-*b*-PI_{10K}-octadecanol-PEG750	OP750	12.6	14.8	27.4	114.6 ± 1.7	38.1 ± 2.2	76.5
PS_{8K}-*b*-$P(E/B)_{25K}$-*b*-PI_{10K}-Octadecanol-PEG850	OP1000	17.1	16.7	33.8	114.4 ± 0.8	35.2 ± 1.8	79.2

[a]Polymer surfaces are named according to the side chains. HP350 represents the PS_{8K}-*b*-$P(E/B)_{25K}$-*b*-PI_{10K} with 1-hexanol and PEG350 in a 50:50 feed ratio. OP1000 represents the PS_{8K}-*b*-$P(E/B)_{25K}$-*b*-PI_{10K} with 1-octadecanol and PEG1000 in a 50:50 feed ratio.

described for the assays with *Ulva*. After 2 h at ∼20 °C on the laboratory bench, three replicate slides of each test coating were washed in seawater without exposure to air (i.e., a submerged wash) to remove cells that had not attached to the surface. The slides were fixed using 2.5% glutaraldehyde in seawater and the density of cells attached to the surfaces was quantified as previously reported.[39]

RESULTS AND DISCUSSION

Polymer Synthesis and Characterization. The amphiphilic SABCs with mixed hydrophobic and hydrophilic side chains were attached to the K3 polymer [PS_{8K}-*b*-$P(E/B)_{25K}$-*b*-PI_{10K}] through Lewis acid-catalyzed ring opening of the epoxidized isoprene block using selected mixtures of hydrophobic aliphatic or PPG alcohols and hydrophilic PEG alcohols (Figure 1). All two-step reactions were conducted using a method similar to that reported previously with perfluoroalkyl and PEG alcohols.[27] Mixed hydrophobic and hydrophilic side chain-derived fluorine-free, amphiphilic SABCs were characterized by FTIR, ^{1}H NMR spectroscopy, and elemental analysis. Alkene protons disappeared completely from the spectrum after the epoxidation reaction, and instead, a significant peak due to protons adjacent to newly formed oxirane rings on the PI block appeared at ∼2.7 ppm. In the FTIR spectrum, a C−O−C stretching peak associated with the epoxide ring appeared at ∼880 cm^{-1}. The C═C absorption from polyisoprene at 1660 and 960 cm^{-1} simultaneously disappeared. Proton peaks of oligoethylene glycol groups at ∼3.6 and 3.4 ppm and aliphatic groups at 0.43 and 0.08 ppm indicate successful attachment of the hydrophilic and hydrophobic side chains, respectively. These findings were also supported by the FTIR results showing a strong O−H stretching peak between 3300 and 3500 cm^{-1}, formed during ring opening of the epoxy group, and a C−O stretching peak at ∼1115 cm^{-1}, formed from the etherification attachment of side chains, for all SABCs. It should also be noted that this functionalization reaction generates hydroxyl groups on the backbone that are hydrophilic in nature. The percentage attachment of side chains in the PS_{8K}-*b*-$P(E/B)_{25K}$-*b*-PI_{10K} precursor is summarized in Tables 1 and 2. The dispersity of the triblock copolymer was found to be 1.06 for the PS-*b*-P(E/B)-*b*-PI precursors and 1.12 for epoxidized PS_{8K}-*b*-$P(E/B)_{25K}$-*b*-PI_{10K}. The dispersities of the amphiphilic SABCs were found to be between 1.14 and 1.46. This variability was due to differences in the efficiency and uniformity of side group attachment. Because reaction between chains did not occur, the lack of uniformity within a batch among polymers having different extents of attachment led to higher dispersity.

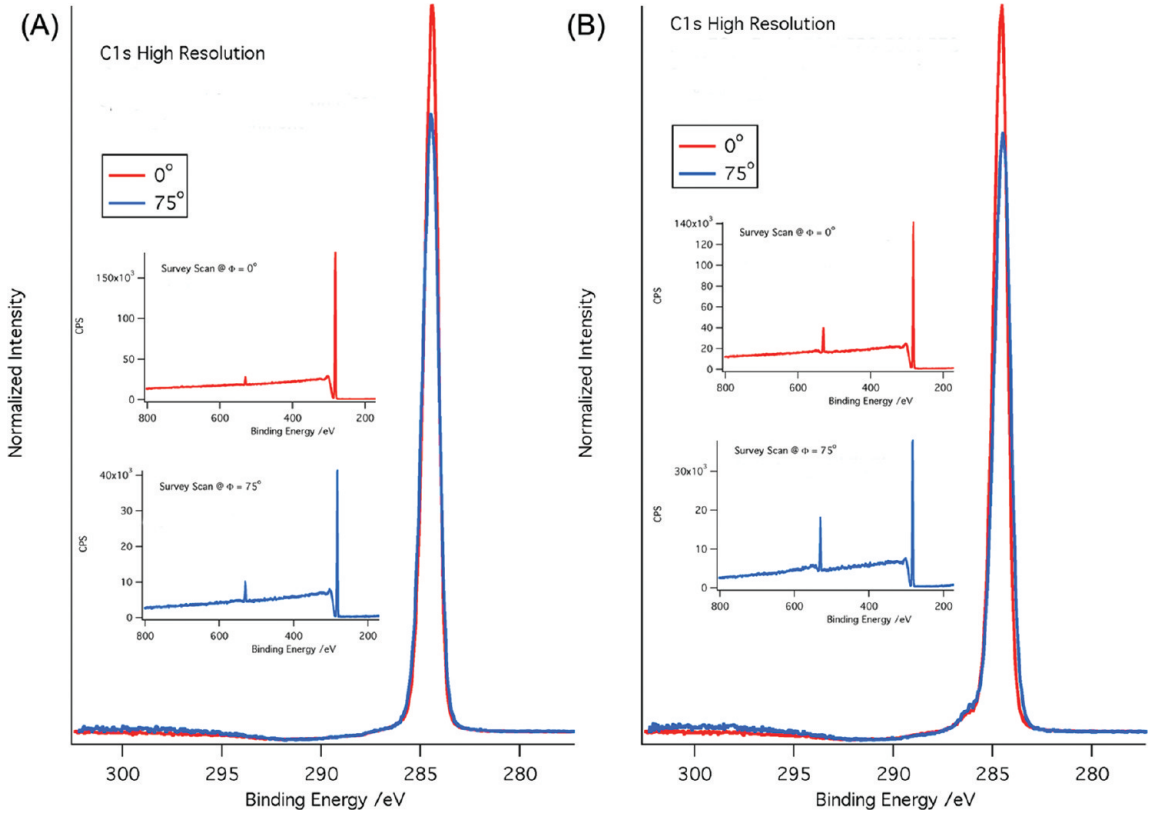

Figure 2. High-resolution C 1s and survey XPS spectra of the amphiphilic SABCs with attached 1-octadecanol/PEG550 (O50P50) (A) and PPG1000/PEG750 (PG50EG50) (B) side chains at electron emission angles of 0° and 75°.

X-ray Photoelectron Spectroscopy (XPS). Figure 2 shows high-resolution C 1s and survey XPS spectra of the amphiphilic SABCs derived from the PS_{8K}-*b*-$P(E/B)_{25K}$-*b*-PI_{10K} precursor with 1-octadecanol/PEG550 and PPG1000/PEG750 side chains with 50:50 feed ratios taken at two different electron emission angles (0° and 75°) relative to the surface normal. The high-resolution spectra are normalized so that the total area under the carbon peaks is equal to unity. The SABCs with attached 1-octadecanol/PEG550 (Figure 2A) and PPG1000/PEG750 (Figure 2B) side chains showed an intense peak from carbon bonded only to C and H near 285 eV, indicating that the surface consists primarily of the P(E/B) block of the SABC. A very weak shoulder at ~286.6 eV from C−O stretching (and a small O peak in the survey scan shown in the inset) suggests the presence of only a few PEG or PPG moieties of the mixed hydrophilic and hydrophobic side chains near the surface. While the 1-octadecanol-derived side chain may contribute to the peak at a binding energy of 285 eV in the sample produced with an equal feed ratio of 1-octadecanol and PEG550, the fact that there is very little evidence of a C−O peak implies that the surface in vacuum is predominately populated by the P(E/B) block. All other amphiphilic SABC surfaces in this study have XPS spectra that are virtually identical to those shown in Figure 2; these show even less evidence of oxygen-containing units near the surface and are provided as Figures 1S−4S of the Supporting Information.

Near-Edge X-ray Absorption Fine Structure (NEXAFS). Figure 3 depicts the normalized C 1s NEXAFS spectra of the amphiphilic SABC surfaces derived from mixed 1-octadecanol/PEG550 (panel A) and PPG1000/PEG750 (panel B) side chains at various feed ratios of the hydrophobic and hydrophilic moieties taken at an angle of 50° between the surface and the soft X-ray beam. The sharp resonance peak near 288 eV can be attributed to the C 1s → σ^*_{C-H} signal. This peak indicates a surface dominated by the low-surface energy poly(ethylene-*ran*-butylene) block, with possible very small contributions from the aliphatic, PPG, and PEG moieties. The very broad peak centered around 292 eV is consistent with the peak from the 1s to σ^*_{C-C} resonance of the P(E/B) block. A very low-intensity peak at 285.5 eV for all the SABC surfaces corresponds to the C 1s → $\pi^*_{C=C}$ resonance from the polystyrene block. These signal intensities are only ~2.5% of the intensity of this peak for pure polystyrene.[43] The normalized C 1s NEXAFS spectra of the PS_{8K}-*b*-$P(E/B)_{25K}$-*b*-PI_{10K} triblock copolymer precursor (K3) and the amphiphilic SABC surfaces derived from mixed 1-hexanol and 1-octadecanol/PEG side chains also show a trend similar to that seen with the SABC surfaces derived from alkyl and PEG side chains (Figure 5S and 6S of the Supporting Information).

Dynamic Water Contact Angle Analysis. Dynamic water contact angle values of the amphiphilic SABCs with grafted 1-octadecanol and PEG550 side chains with different feed ratios are summarized in Table 1. The following dynamic water contact angles of the control surfaces were observed: for the SEBS, $\theta_{w,ad}$ = 129.7° (advancing) and $\theta_{w,re}$ = 56.5° (receding), for the PS_{8K}-*b*-$P(E/B)_{25K}$-*b*-PI_{10K} precursor, $\theta_{w,ad}$ = 116.3° (advancing) and $\theta_{w,re}$ = 59.4° (receding). The high advancing and receding water contact angles can be attributed to the hydrophobic blocks in the SEBS and PS_{8K}-*b*-$P(E/B)_{25K}$-*b*-PI_{10K} precursor polymers. The amphiphilic SABC surfaces with grafted 1-octadecanol and PEG550 side chains have advancing contact angles ranging from 119.9° to 115.4° and receding contact angles ranging from 42.7° to 32.3°. Advancing and receding contact angles on these SABC surfaces decrease as the

dx.doi.org/10.1021/bm300363g | *Biomacromolecules* 2012, 13, 1864−1874

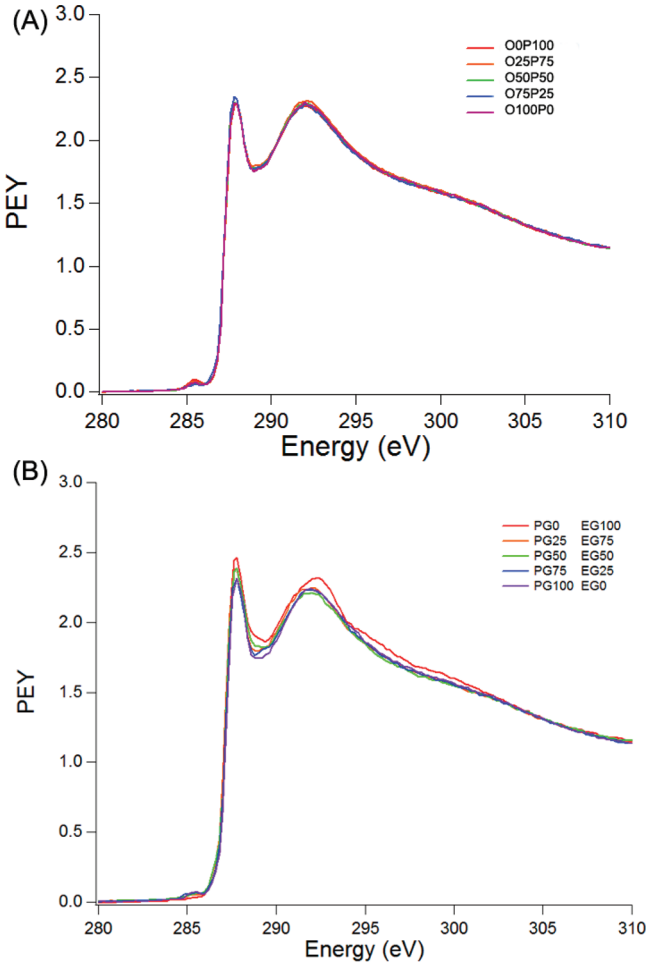

Figure 3. NEXAFS spectra of the amphiphilic SABCs with attached 1-octadecanol/PEG550 (A) and PPG1000/PEG750 (B) side chains at an angle of 50° between the surface and the soft X-ray beam and an electron emission angle relative to the sample normal of 4°.

content of PEG550 to octadecanol is increased. This large difference between the advancing and receding contact angles corresponds to a large contact angle hysteresis. The high contact angle hysteresis on all SABC surfaces after hydration suggests that despite strong evidence from XPS and NEXAFS in vacuum that the PEG groups do not populate the surface, surface reorganization of the triblock copolymer occurs to expose the hydrophilic PEG side chains to a water environment as seen previously for other amphiphilic surfaces.[22,27,32] One of the purposes of this study was to examine systematically the effects of aliphatic and PEG segment length on this reorganization.

Table 2 shows the dynamic water contact angles of the amphiphilic SABC surfaces derived from various alkyl and PEG side chains. As the length of the PEG unit increased, the advancing and receding contact angles tended to decrease. The contact angles also tended to decrease as the length of the alkyl chain decreased. A high contact angle hysteresis is also seen for these SABC surfaces.

The dynamic water contact angles of the amphiphilic SABC surfaces derived from PPG1000 and PEG750 side chains as a function of the feed ratio are summarized in Table 1S of the Supporting Information. For the SABC surfaces, the advancing and receding contact angles depended on the amount of hydrophobic PPG and hydrophilic PEG side chains. The advancing contact angle decreased from 107.7° for the block copolymer that has only PPG side chains to 85.2° for the block copolymer with only PEG side chains, and the corresponding receding contact angle decreased from 30.7° to 16.7°. The initial presence on the surface of the P(E/B) block is responsible for the higher advancing contact angle. All the polymers showed a strong contact angle hysteresis as seen with the other amphiphilic SABC surfaces in Tables 1 and 2. These contact angles correlate with the results of protein adsorption; the settlement and detachment of *Ulva* and *Navicula* will be discussed below.

Captive Air-Bubble Contact Angle Analysis. The captive air-bubble contact angles measured underwater on the amphiphilic SABC surfaces derived from mixed alkyls and PEG side chains are shown in Figure 4. The captive air-bubble

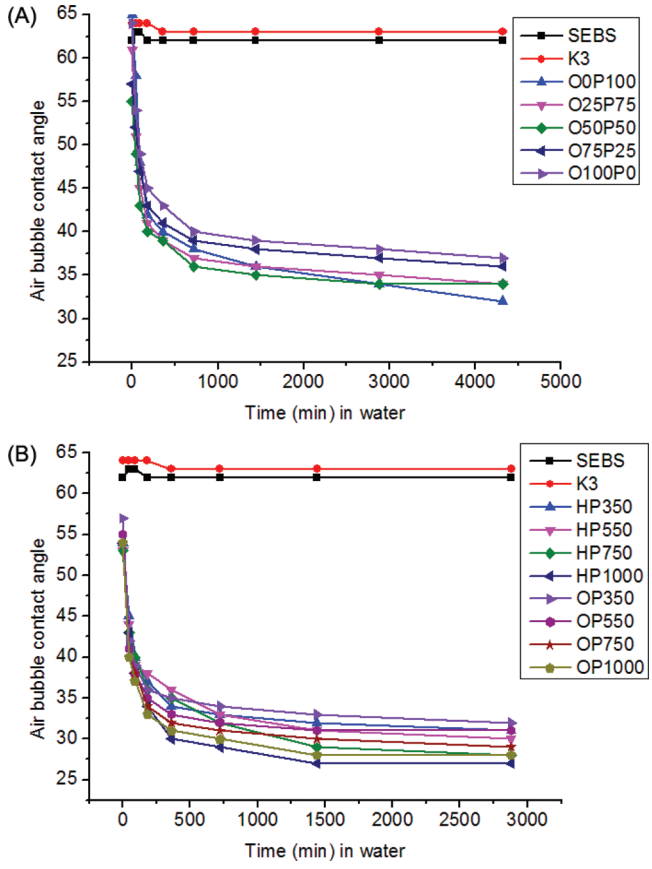

Figure 4. Captive air-bubble contact angles under water on SABCs (A) with grafted 1-octadecanol/PEG550 side chains at various feed ratios and (B) with 1-hexanol and/or 1-octadecanol/PEG350, -550, -750, and -1000 side chains.

contact angles on hydrophobic SEBS and K3 control surfaces are constant following immersion, while the contact angles on the amphiphilic SABC surfaces derived from 1-octadecanol and PEG550 side chains (Figure 4A) as well as 1-hexanol/1-octadecanol and PEG side chains (Figure 4B) decrease as a function of time under water. The captive air-bubble contact angles were generally lower with a higher PEG content. This could be due to the presence of more hydrophilic PEG units on the surface. There are two distinct regions in the plot: an initial rapid decrease in contact angles within the first 3 h and then a slow decrease in contact angles over a period of 2 or 3 days. The air-bubble contact angle of the O100P0 surface that had

dx.doi.org/10.1021/bm300363g | *Biomacromolecules* 2012, 13, 1864−1874

only hydrophobic side chains decreased over time because of the presence of hydroxyl groups on the polymer backbone. The initial contact angle under water at 0 min shows a similar value for all surfaces (SEBS, 62°; K3, 64°; O0P100, 65°; O25P75, 61°; O50P50, 55°; O75P25, 57°; O100P0, 64°). In particular, the O0P100 surface shows an initial contact angle of 65° at 0 min. It suggests that the annealed dry surfaces are initially dominated by hydrophobic groups. However, these surfaces are reconstructed under water over time and become dominated by hydrophilic groups. In other words, the decrease of the contact angle under water for all SABC surfaces suggests that the reorganization of the surfaces exposes the hydrophilic hydroxyl group and PEG side chain to a water environment. Air-bubble contact angle measurements of the amphiphilic SABC surfaces derived from PPG and PEG side chains show trends similar to that seen with the amphiphilic SABC surfaces derived from alkyl and PEG side chains (Figure 7S of the Supporting Information).

Atomic Force Microscopy (AFM). To characterize the change in the morphology of the surfaces upon exposure to an aqueous environment, the surfaces were immersed in water for 7 days and analyzed by AFM. The surface features were compared with those of the dry surfaces. Figure 5 shows the AFM phase images of the amphiphilic SABC surfaces derived from mixed PEG750 and PPG1000 side chains at various feed ratios: PG0EG100 (A), PG25EG75 (B), PG50EG50 (C), PG75EG25 (D), and PG100EG0 (E) after dry annealing and PG0EG100 (F), PG25EG75 (G), PG50EG50 (H), PG75EG25 (I), and PG100EG0 (J) after immersion under water for 7 days. All amphiphilic SABC surfaces showed a planar cylindrical morphology. The size of the phase domain on dry surfaces is ~25−35 nm. All the surfaces retain the cylindrical morphology upon immersion in water. However, the size of the phase domain on the amphiphilic SABC surfaces increased from 25−35 to 60−100 nm after immersion in water. The change in the scale of the morphology is probably due to the swelling of the hydrophilic PEG moiety in water. This result demonstrates reorganization of the P(E/B) block and the side chains on the functionalized end block of the SABCs under water and indicates that the PEG units are probably exposed to water. The AFM phase images on the amphiphilic SABC surfaces derived from alkyl and PEG side chains after dry annealing are shown in Figure 8S of the Supporting Information. The size of the phase domain on dry surfaces is ~30 nm. While no systematic investigation of the morphology under water by AFM was conducted, a comparison of the dry surface and the wet surface (AFM image under water) of the SABC with grafted 1-octadecanol and PEG750 side chains produced using a 50:50 feed ratio shows changes in morphology (Figure 9S of the Supporting Information) similar to those shown in Figure 5.

Protein Adsorption Study. Figure 6 shows the fluorescence intensities of adsorbed BSA on the amphiphilic SABC surfaces derived from mixed 1-octadecanol and PEG550 side chains (A) and mixed 1-hexanol/1-octadecanol and PEG side chains (B). BSA shows high adsorption on the hydrophobic SEBS control and the PS_{8K}-*b*-$P(E/B)_{25K}$-*b*-PI_{10K} triblock copolymer precursor (K3) surfaces compared to the amphiphilic SABC surfaces. The amphiphilic SABC surfaces were found to strongly resist BSA adsorption. The fluorescence intensity on the amphiphilic SABC surfaces was ~10-fold lower than that on the SEBS control surface. With the increase in the content of PEG in the amphiphilic SABC surfaces, the surfaces become more resistant to BSA as depicted in Figure 6A. All amphiphilic SABC surfaces containing the various alkyl and PEG side chains are also similarly resistant to BSA (Figure 6B). These results clearly demonstrate that amphiphilic SABCs with grafted mixed hydrophilic and hydrophobic side chains are resistant to protein adsorption.

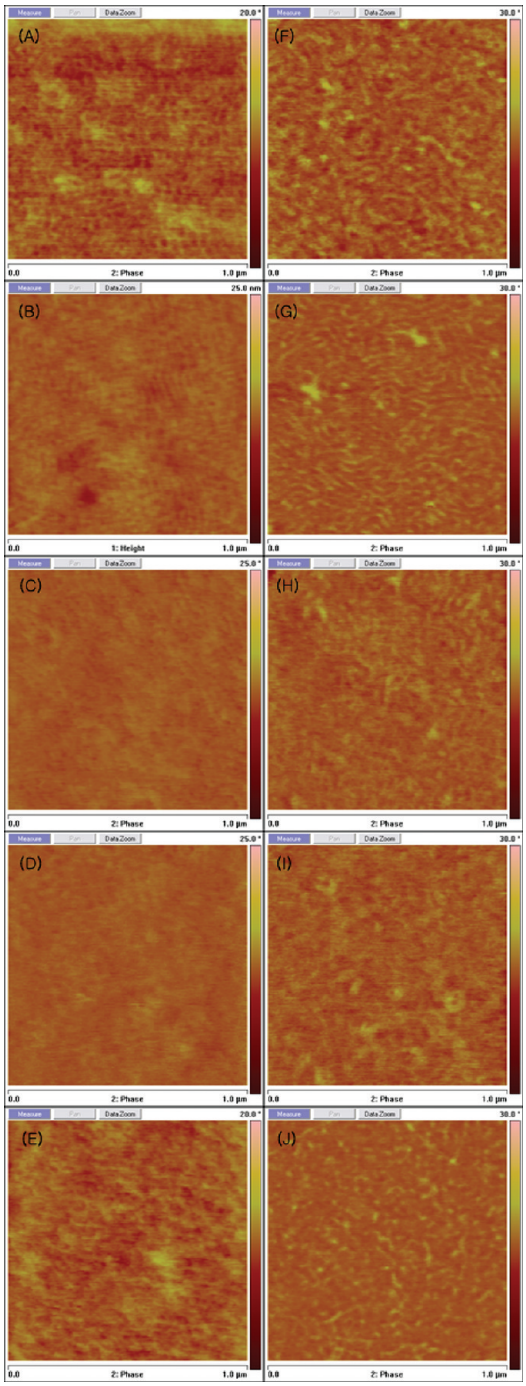

Figure 5. AFM phase images of the amphiphilic SABCs with grafted PPG1000 and PEG750 side chains at various feed ratios: PG0EG100 (A), PG25EG75 (B), PG50EG50 (C), PG75EG25 (D), and PG100EG0 (E) after dry annealing; AFM phase images of the amphiphilic SABCs with grafted PPG1000 and PEG750 side chains at various feed ratios: PG0EG100 (F), PG25EG75 (G), PG50EG50 (H), PG75EG25 (I), and PG100EG0 (J) after immersion under water for 7 days. PG*x*EG*y* represents the PS_{8K}-*b*-$P(E/B)_{25K}$-*b*-PI_{10K} with an *x* feed ratio of PPG1000 and a *y* feed ratio of PEG750.

dx.doi.org/10.1021/bm300363g | *Biomacromolecules* 2012, 13, 1864−1874

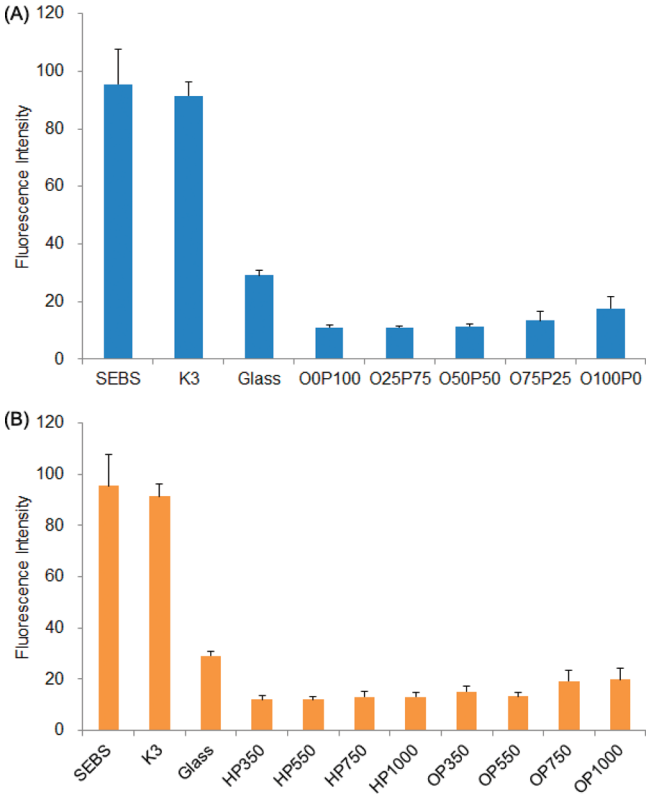

Figure 6. Fluorescence intensities of the adsorbed BSA on SABC surfaces with grafted with various feed ratios of 1-octadecanol/PEG550 (A) and 1-hexanol and/or 1-octadecanol/PEG350, -550, -750, and -1000 side chains.

Release of *Ulva* Sporelings. Attached zoospores germinated, and after they had been cultured for 7 days, green lawns of sporelings (young plants) covered all test surfaces. The percentage removal of sporelings from the SABC surfaces derived from mixed 1-octadecanol and PEG550 side chains (A), mixed 1-hexanol and PEG side chains (B), and mixed 1-octadecanol and PEG side chains (C) at a range of applied water jet pressures is shown in Figure 7. Sporelings were removed from the PDMS standard surface at low water jet pressures, reflecting the good fouling-release properties of this low-surface energy elastomer.[22,44] Interestingly, all SABC surfaces derived from mixed alkyl and PEG side chains demonstrated a release of sporelings superior to that of the PDMS standard and K3 control surfaces. Additionally, most of the sporelings (~100%) were released from all SABC surfaces at relatively low water pressures (~30 kPa). The fouling-release performance improved remarkably after chemical modification with mixed hydrophilic and hydrophobic side chains from the PS_{8K}-*b*-$P(E/B)_{25K}$-*b*-PI_{10K} triblock copolymer precursor (K3). These observations demonstrate that mixed amphiphilic side chains play an important role on the surface in the aqueous environment. Furthermore, the results suggest that excellent fouling-release behavior can be achieved for mixed aliphatic and PEG-based amphiphilic materials that do not incorporate environmentally unfriendly fluorinated groups, even though in a dry environment (XPS spectra) there is no sign of PEG groups on the surface.

The detachment at a range of water jet impact pressures of sporelings from PDMS, K3, and amphiphilic SABC surfaces produced using different compositions of PPG1000 and

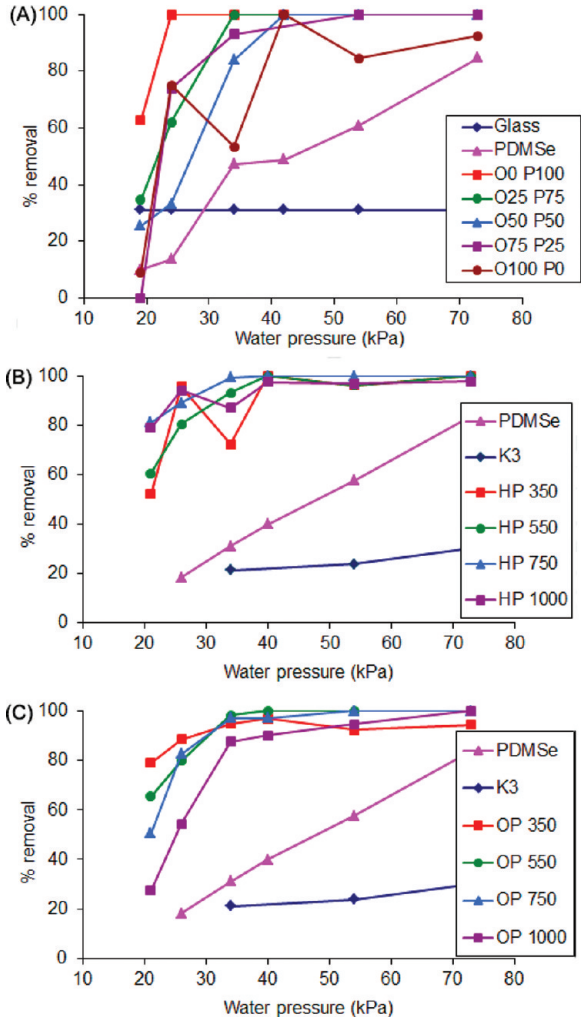

Figure 7. Detachment of sporelings of *Ulva* from the amphiphilic SABC surface with grafted mixed 1-octadecanol/PEG550 (as the feed ratio) (A), 1-hexanol/PEG (B), and 1-octadecanol/PEG (C) side chains. Coated slides were exposed to the water jet over a range of water pressures. One slide was used at each pressure.

PEG750 side chains are shown in Figure 8. Sporelings were removed from the amphiphilic SABC surfaces containing PPG25−75 at water jet pressures lower than the PDMS standard. The adhesion strength on the PPG0 and PPG100

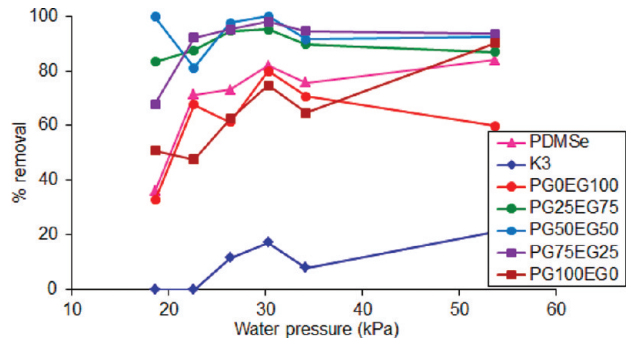

Figure 8. Detachment of sporelings of *Ulva* from the SABC surfaces derived from PPG/PEG side chains. Coated slides were exposed to the water jet over a range of water pressures. One slide was used at each pressure.

dx.doi.org/10.1021/bm300363g | *Biomacromolecules* 2012, 13, 1864−1874

coatings was slightly lower than those on the others, suggesting that blends of the two side chains produced the most effective formulations.

Attachment of Cells of the Diatom *Navicula*. Attachment of cells of the diatom *Navicula* was also evaluated on the amphiphilic SABC surfaces. Figure 9 shows the density of attached *Navicula* cells after the slides had been washed on the SABC surfaces derived from mixed 1-octadecanol and PEG550 side chains as the feed ratio (A) and mixed various alkyl and PEG side chains (B). The density of attached cells decreased as the content of the PEG unit in the side chains increased (Figure 9A). These results show that fewer diatom cells were able to remain attached to the hydrophilic surfaces when exposed to the hydrodynamic forces associated with washing the slides compared to other types of surfaces.[45,46] These data followed the same trend as the results of the protein adsorption experiments. More *Navicula* cells were attached to the hydrophobic PDMS standard and K3 control surfaces, but few cells were present after washing on most of the amphiphilic SABC surfaces with grafted mixed alkyl and PEG side chains (Figure 9B). On the basis of these results, we suggest that the amphiphilic SABC surfaces derived from mixed hydrocarbon and PEG side chains are ideal surfaces for minimizing the adhesion of the cells of the diatom *Navicula*.

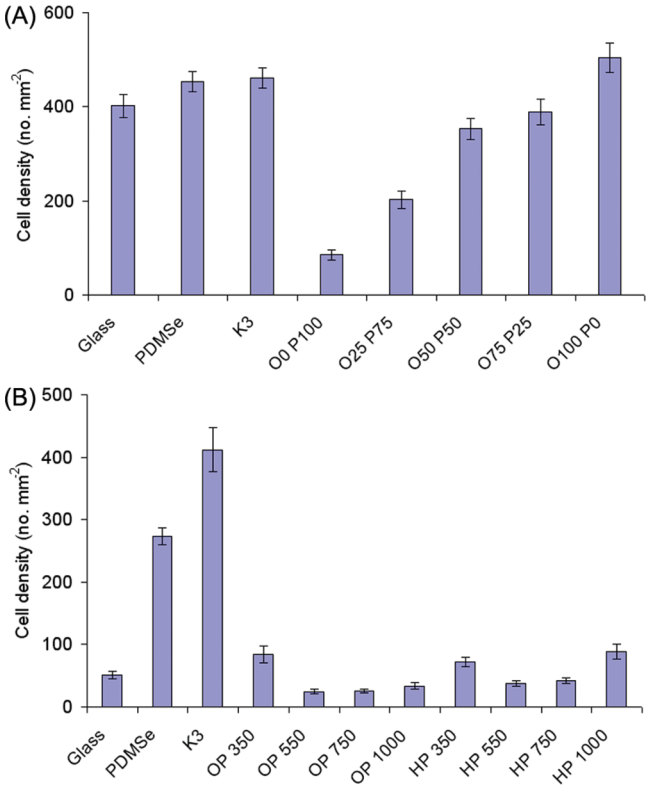

Figure 9. Density of attached *Navicula* on SABC surfaces with grafted 1-octadecanol/PEG550 (A) and 1-hexanol and/or 1-octadecanol/PEG350, -550, -750, and -1000 (B) side chains after washing. Each point is the mean from 90 counts on three replicate slides. Bars show 95% confidence limits.

CONCLUSION

Coatings based on a combination of hydrophobic hydrocarbon and hydrophilic PEO units were prepared by modifying the polyisoprene (PI) block of a PS_{8K}-*b*-$P(E/B)_{25K}$-*b*-PI_{10K} triblock copolymer. These materials were shown to be more effective in resisting fouling by the green alga *Ulva* and cells of the diatom *Navicula* than either a PDMS standard material or the PS_{8K}-*b*-$P(E/B)_{25K}$-*b*-PI_{10K} triblock copolymer precursor. While similar in fouling resistance to previously studied mixed surfaces that combined perfluorocarbons and PEO groups, these new fluorine-free materials initially form surfaces that show no sign of the hydrophilic PEG or even PPG moieties when characterized by XPS and NEXAFS. Nevertheless, the air-bubble contact angle data, AFM measurements, and biofouling results indicate that these surfaces must be reconstructed substantially to bring the PEG to the surface. The results are therefore qualitatively different from those for previously reported mixed surfaces with perfluorinated and PEG side groups. Antifouling and fouling-release properties were found to depend on the proportion of the hydrophilic PEG groups incorporated into the SABC surfaces. These amphiphilic SABCs are also very resistant to the adsorption of bovine serum albumin (BSA), which was used as a standard test protein. As a result, it has been demonstrated that the fluorine-free, amphiphilic SABCs derived from mixed alkyl and PEG side chains are excellent candidates for marine antifouling and fouling-release coatings as alternatives to fluorinated materials as they have reduced potential for a negative environmental impact.

ASSOCIATED CONTENT

Supporting Information

Dynamic water contact angles of the amphiphilic triblock copolymer surfaces with grafted PPG1000 and PEG750 side chains as the feeding ratio, high-resolution C 1s and survey XPS spectra of all amphiphilic SABCs at electron emission angles of 0° and 75°, NEXAFS spectra of the PS_{8K}-*b*-$P(E/B)_{25K}$-*b*-PI_{10K} triblock copolymer precursor (K3) and the amphiphilic SABCs with attached 1-hexanol/PEG and 1-octadecanol/PEG side chains, captive air-bubble contact angles under water on SABCs with grafted PPG1000 and PEG550 in a 50:50 feed ratio, AFM phase images of the amphiphilic SABCs with grafted 1-octadecanol and PEG550 side chains at various feed ratios [O0P100 (A), O25P75 (B), O50P50 (C), O75P25 (D), and O100P0 (E) after dry annealing], AFM phase images of the amphiphilic SABCs with grafted 1-octadecanol and PEG750 side chains at 50:50 feed ratios after dry annealing (A) and after immersion under water for 7 days (B), and settlement densities of *Ulva* spores on SABC surfaces with grafted 1-octadecanol/PEG550 (A) and 1-hexanol and/or 1-octadecanol/PEG350, -550, -750, and -1000 side chains. This material is available free of charge via the Internet at http://pubs.acs.org.

AUTHOR INFORMATION

Corresponding Author

*Department of Materials Science and Engineering, 310 Bard Hall, Cornell University, Ithaca, NY 14853. Phone: (607) 255-8417. Fax: (607) 255-2365. E-mail: cko3@cornell.edu.

Notes

The authors declare no competing financial interest.

ACKNOWLEDGMENTS

This work was supported by the Office of Naval Research (ONR) through Grants N00014-02-1-0170 (C.K.O. and E.J.K.) and N00014-08-1-0010 (J.A.C. and M.E.C.). Additional support was provided by the U.S. Department of Defense's

Strategic Environmental Research and Development Program (SERDP), via Grant WP #1454. This work was also partially supported by NanoSurfaces, Inc. (SHS). Additionally, E.J.K. and M.D.D. acknowledge partial support from the National Science Foundation (NSF) Polymers Program (DMR-0704539) as well as the use of central facilities funded by the NSF-MRSEC program (UCSB MRL, DMR-1121053).

REFERENCES

(1) Schultz, M. P.; Bendick, J. A.; Holm, E. R.; Hertel, W. M. *Biofouling* **2011**, *27*, 87−98.
(2) Schultz, M. P. *Biofouling* **2007**, *23*, 331−333.
(3) Finnie, A.; Williams, D. N. In *Paint and Coatings Technology for the Control of Marine Fouling in Biofouling*; Durr, S., Thomason, J. C., Eds.; Wiley-Blackwell: Chichester, U.K., 2010; p 429.
(4) Thomas, K. V.; Brooks, S. *Biofouling* **2010**, *26*, 73−88.
(5) Yebra, D. M.; Kiil, S.; Dam-Johansen, K. *Prog. Org. Coat.* **2004**, *50*, 75−104.
(6) Genzer, J.; Efimenko, K. *Biofouling* **2006**, *22*, 339−360.
(7) Chambers, L. D.; Stokes, K. R.; Walsh, F. C.; Wood, R. J. K. *Surf. Coat. Technol.* **2006**, *201*, 3642−3652.
(8) Vladkova, T. *J. Univ. Chem. Technol. Metall.* **2007**, *42*, 239−256.
(9) Krishnan, S.; Weinman, C. J.; Ober, C. K. *J. Mater. Chem.* **2008**, *18*, 3405−3413.
(10) Callow, J. A.; Callow, M. E. *Nat. Commun.* **2011**, *2*, 244.
(11) Scardino, A. J.; DeNys, R. *Biofouling* **2011**, *27*, 73−86.
(12) Prime, K. L.; Whitesides, G. M. *J. Am. Chem. Soc.* **1993**, *115*, 10714−10721.
(13) Ma, H.; Hyun, J.; Stiller, P.; Chilkoti, A. *Adv. Mater.* **2004**, *16*, 338−341.
(14) Schilp, S.; Kueller, A.; Rosenhahn, A.; Grunze, M.; Pettitt, M. E.; Callow, M. E.; Callow, J. A. *Biointerphases* **2007**, *2*, 143−150.
(15) Marabotti, I.; Morelli, A.; Orsini, L. M.; Martinelli, E.; Galli, G.; Chiellini, E.; Lien, E. M.; Pettitt, M. E.; Callow, J. A.; Conlan, S. L.; Mutton, R. J.; Clare, A. S.; Kocijan, A.; Donik, C.; Jenko, M. *Biofouling* **2009**, *25*, 481−493.
(16) Sommer, S.; Ekin, A.; Webster, D. C.; Stafslien, S.; Daniels, J.; Van Der Wal, L. J.; Thompson, S. E. Y.; Callow, M. E.; Callow, J. A. *Biofouling* **2010**, *26*, 961−972.
(17) Magin, C. M.; Long, C. J.; Cooper, S. P.; Ista, L. K.; Lopez, G. P.; Brennan, A. B. *Biofouling* **2010**, *26*, 719−727.
(18) Yarbrough, J. C.; Rolland, J. P.; DeSimone, J. M.; Callow, M. E.; Finlay, J. A.; Callow, J. A. *Macromolecules* **2006**, *39*, 2521−2528.
(19) Youngblood, J. P.; Andruzzi, L.; Ober, C. K.; Hexemer, A.; Kramer, E. J.; Callow, J. A.; Finlay, J. A.; Callow, M. E. *Biofouling* **2003**, *19*, 91−98.
(20) Beigbeder, A.; Degee, P.; Conlan, S. L.; Mutton, R. J.; Clare, A. S.; Pettitt, M. E.; Callow, M. E.; Callow, J. A.; Dubois, P. *Biofouling* **2008**, *24*, 291−302.
(21) Wynne, K. J.; Swain, G. W.; Fox, R. B.; Bullock, S.; Ulik, J. *Biofouling* **2000**, *16*, 277−288.
(22) Krishnan, S.; Wang, N.; Ober, C. K.; Finlay, J. A.; Callow, M. E.; Callow, J. A.; Hexemer, A.; Sohn, K. E.; Kramer, E. J.; Fischer, D. A. *Biomacromolecules* **2006**, *7*, 1449−1462.
(23) Gudipati, C. S. F.; Callow, J. A.; Callow, M. E.; Wooley, K. L. *Langmuir* **2005**, *21*, 3044−3053.
(24) Krishnan, S.; Ayothi, R.; Hexemer, A.; Finlay, J. A.; Sohn, K. E.; Perry, R.; Ober, C. K.; Kramer, E. J.; Callow, M. E.; Callow, J. A.; Fischer, D. A. *Langmuir* **2006**, *22*, 5075−5086.
(25) Weinman, C. J.; Finlay, J. A.; Park, D.; Paik, M. Y.; Krishnan, S.; Sundaram, H. S.; Dimitriou, M.; Sohn, K. E.; Callow, M. E.; Callow, J. A.; Handlin, D. L.; Willis, C. L.; Kramer, E. J.; Ober, C. K. *Langmuir* **2009**, *25*, 12266−12274.
(26) Martinelli, E.; Agostini, S.; Galli, G.; Chiellini, E.; Glisenti, A.; Pettiitt, M. E.; Callow, M. E.; Callow, J. A.; Graf, K.; Bartels, F. W. *Langmuir* **2008**, *24*, 13138−13147.
(27) Park, D.; Weinman, C. J.; Finlay, J. A.; Fletcher, B. R.; Paik, M. Y.; Sundaram, H. S.; Dimitriou, M. D.; Sohn, K. E.; Callow, M. E.; Callow, J. A.; Handlin, D. L.; Willis, C. L.; Fisher, D. A.; Kramer, E. J.; Ober, C. K. *Langmuir* **2010**, *26*, 9772−9781.
(28) Martinelli, E.; Suffredini, M.; Galli, G.; Glisenti, A.; Pettitt, M. E.; Callow, M. E.; Callow, J. A.; Williams, D.; Lyall, G. *Biofouling* **2011**, *27*, 529−541.
(29) Kannan, K.; Koistinen, J.; Beckmen, K.; Evans, T.; Gorzelany, J. F.; Hansen, K. J.; Jones, O. P. D.; Helle, E.; Nyman, M.; Giesy, J. P. *Environ. Sci. Technol.* **2001**, *35*, 1593−1598.
(30) Martin, J. W.; Mabury, S. A.; Solomon, K. R.; Muir, D. C. G. *Environ. Toxicol. Chem.* **2003**, *22*, 196−204.
(31) Olsen, G. W.; Huang, H. Y.; Helzlsouer, K. J.; Hansen, K. J.; Butenhoff, J. L.; Mandel, J. H. *Environ. Health Perspect.* **2005**, *113*, 539−545.
(32) Cho, Y.; Sundaram, H. S.; Weinman, C. J.; Paik, M. Y.; Dimitriou, M. D.; Finlay, J. A.; Callow, M. E.; Callow, J. A.; Kramer, E. J.; Ober, C. K. *Macromolecules* **2011**, *44*, 4783−4792.
(33) Li, X.; Andruzzi, L.; Chiellini, E.; Galli, G.; Ober, C. K.; Hexemer, A.; Kramer, E. J.; Fischer, D. A. *Macromolecules* **2002**, *35*, 8078−8087.
(34) Xiang, M. L.; Li, X. F.; Ober, C. K.; Char, K.; Genzer, J.; Sivaniah, E.; Kramer, E. J.; Fischer, D. A. *Macromolecules* **2000**, *33*, 6106−6119.
(35) Sohn, K. E.; Dimitriou, M. D.; Genzer, J.; Fischer, D. A.; Hawker, C. J.; Kramer, E. J. *Langmuir* **2009**, *25*, 6341−6348.
(36) Krishnan, S.; Ward, R. J.; Hexemer, A.; Sohn, K. E.; Lee, K. L.; Angert, E. R.; Fischer, D. A.; Kramer, E. J.; Ober, C. K. *Langmuir* **2006**, *22*, 11255−11266.
(37) Schumacher, J. F.; Carman, M. L.; Estes, T. G.; Feinberg, A. W.; Wilson, L. H.; Callow, M. E.; Callow, J. A.; Finlay, J. A.; Brennan, A. B. *Biofouling* **2007**, *23*, 55−62.
(38) Callow, M. E.; Callow, J. A.; Pickett-Heaps, J. D.; Wetherbee, R. *J. Physiol.* **1997**, *33*, 938−947.
(39) Callow, M. E.; Jennings, A. R.; Brennan, A. B.; Seegert, C. E.; Gibson, A.; Wilson, L.; Feinberg, A.; Baney, R.; Callow, J. A. *Biofouling* **2002**, *18*, 237−245.
(40) Chaudhury, M. K.; Finlay, J. A.; Chung, J. Y.; Callow, M. E.; Callow, J. A. *Biofouling* **2005**, *21*, 41−48.
(41) Casse, F.; Ribeiro, E.; Ekin, A.; Webster, D. C.; Callow, J. A.; Callow, M. E. *Biofouling* **2007**, *23*, 267−276.
(42) Finlay, J. A.; Callow, M. E.; Schultz, M. P.; Swain, G. W.; Callow, J. A. *Biofouling* **2002**, *18*, 251−256.
(43) Dimitriou, M. D.; Zholi, Z.; Yoo, H.-S.; Killops, K. L.; Finlay, J. A.; Cone, G.; Sundaram, H. S.; Lynd, N. A.; Barteau, K. P.; Campos, L. M.; Fisher, D. A.; Callow, M. E.; Callow, J. A.; Ober, C. K.; Hawker, C. J.; Kramer, E. J. *Langmuir* **2011**, *27*, 13762−13772.
(44) Finlay, J. A.; Krishnan, S.; Callow, M. E.; Callow, J. A.; Dong, R.; Asgill, N.; Wong, K.; Kramer, E. J.; Ober, C. K. *Langmuir* **2008**, *24*, 503−510.
(45) Holland, R.; Dugdale, T. M.; Wetherbee, R.; Brannan, A. B.; Finlay, J. A.; Callow, M. E.; Callow, J. A. *Biofouling* **2004**, *20*, 323−329.
(46) Finlay, J. A.; Bennett, S. M.; Brewer, L. H.; Sokolova, A.; Clay, G.; Gunari, N.; Meyer, A. E.; Walker, G. C.; Wendt, D. E.; Callow, M. E.; Callow, J. A.; Detty, M. R. *Biofouling* **2010**, *26*, 657−666.